An interferometric complementarity experiment in a bulk nuclear magnetic resonance ensemble

2003 J. Phys. A: Math. Gen. 36 2555

(http://iopscience.iop.org/0305-4470/36/10/315)

INSTITUTE OF PHYSICS PUBLISHING JOURNAL OF PHYSICS A: MATHEMATICAL AND GENERAL

J. Phys. A: Math. Gen. **36** (2003) 2555–2563 PII: S0305-4470(03)52203-X

An interferometric complementarity experiment in a bulk nuclear magnetic resonance ensemble

Xinhua Peng[1], **Xiwen Zhu**[1], **Ximing Fang**[1,2], **Mang Feng**[1], **Maili Liu**[1] **and Kelin Gao**[1]

[1] State Key Laboratory of Magnetic Resonance and Atomic and Molecular Physics, Wuhan Institute of Physics and Mathematics, The Chinese Academy of Sciences, Wuhan 430071, People's Republic of China
[2] Department of Physics, Hunan Normal University, Changsha 410081, People's Republic of China

E-mail: xhpeng@wipm.ac.cn

Received 9 August 2002
Published 26 February 2003
Online at stacks.iop.org/JPhysA/36/2555

Abstract

We have experimentally demonstrated the interferometric complementarity, which relates the distinguishability D quantifying the amount of which-way (WW) information to the fringe visibility V characterizing the wave feature of a quantum entity, in a bulk ensemble by nuclear magnetic resonance (NMR) techniques. We are primarily concerned about the intermediate cases: partial fringe visibility and incomplete WW information. We propose a quantitative measure of D by an alternative geometric strategy and investigate the relation between D and entanglement. By measuring D and V independently, it turns out that the duality relation $D^2 + V^2 = 1$ holds for pure quantum states of the markers.

PACS numbers: 03.65.Ud, 03.67.−a

1. Introduction

Bohr complementarity [1] expresses the fact that quantum systems possess properties that are equally real but mutually exclusive. This is often illustrated by means of Young's two-slit interference experiment, where 'the observation of an interference pattern and the acquisition of which-way (WW) information are mutually exclusive' [2]. As stated by Feynman, the two-slit experiment 'has in it the heart of quantum mechanics. In reality, it contains the only mystery' [3]. The complementarity is often superficially identified with the 'wave–particle duality of matter'. Because of its tight association with the interference experiment, the terms 'interferometric duality' or 'interferometric complementarity' are more preferable. Two extreme cases, 'full WW information and no fringes when measuring the population of quantum states' and 'perfect fringe visibility and no WW information' have been clarified

in textbooks and demonstrated with many different kinds of quantum objects including photons [4], electrons [5], neutrons [6], atoms [7] and nuclear spins in a bulk ensemble with nuclear magnetic resonance (NMR) techniques [8]. In [8], we further proved theoretically and experimentally that full WW information is exclusive with population fringes but compatible with coherence patterns.

In order to describe the duality in the intermediate regime 'partial fringe visibility and partial WW information', quantitative measures for both the fringe visibility V and WW information are required. The definition of the former is the usual one. In variants of two-slit experiments, different WW detectors or markers, such as microscopic slit and micromaser, are used to label the way in which the quantum entity evolves. A quantitative approach to WW knowledge was first given by Wootters and Zurek [11], and then by Bartell [12]. Some relevant inequalities to quantify the interferometric duality can be found in a number of other publications [2, 13–16]. Among them, Englert [2] presented definitions of the predictability P and the distinguishability D to quantify how much WW information is stored in the marker, and derived an inequality $D^2+V^2 \leqslant 1$ at the intermediate stage which puts a bound on D when given a certain fringe visibility V. Although the quantitative aspects of the interferometric complementarity have been discussed in a number of theoretical papers, there are just a few experimental studies, i.e., the neutron experiments [17, 18], the photon experiments [19, 20] and the atom interferometer [21]. Recently, a complementarity experiment with an interferometer at the quantum–classical boundary [22] was also described.

In this paper, we experimentally investigate the interferometric complementarity of the ensemble-averaged spin states of one of two kinds of nuclei in NMR sample molecules for the intermediate situations. We follow our approach detailed in [8], but use two non-orthogonal spin states of another nuclei in the sample molecules as the path markers. By entangling the observed spin with the marker one, the interference is destroyed because it is in principle possible to determine the states the observed spin possesses by performing a suitable measurement of the marker one [2]. However, in this paper, an alternative geometric strategy of measuring D is given and the relationship between D and the entanglement of the spin states is clarified. And finally the duality relation $D^2 + V^2 = 1$ for various values of D and V is demonstrated.

2. Scheme and definition

Our experimental scheme can be illustrated by a Mach–Zehnder interferometer (shown in figure 1), a modified version of the two-slit experiment. The observed and marker quantum objects, represented by B and A, respectively, compose a bipartite quantum system BA. Suppose the input state of BA to be $|\psi_0\rangle = |0\rangle_B|0\rangle_A \equiv |00\rangle$, with $|0\rangle$ being one of two orthonormal bases $|0\rangle$ and $|1\rangle$ of B and A. Firstly, a beam splitter (BS) splits $|0\rangle_B$ into $\frac{1}{\sqrt{2}}(|0\rangle_B + |1\rangle_B)$, meaning that the observed system B evolves along the two paths $|0\rangle_B$ and $|1\rangle_B$ simultaneously with equal probabilities. In the meantime, path markers (PM) label the different paths $|0\rangle_B$ and $|1\rangle_B$ with the marker states $|m_+\rangle_A$ and $|m_-\rangle_A$ respectively. The joint action of the BS and PM denoted by operation U_1, thus transforms $|\psi_0\rangle$ into

$$|\psi_1\rangle = \tfrac{1}{\sqrt{2}}(|0\rangle_B|m_+\rangle_A + |1\rangle_B|m_-\rangle_A). \tag{1}$$

Secondly, phase shifters (PS) add a relative phase difference between the two paths, which are then combined into the output state $|\psi_2\rangle$ by a beam merge (BM). The joint action of the PS and BM, which is applied solely on B is accomplished by a unitary operation

$$U_2 = \frac{1}{\sqrt{2}}\begin{pmatrix} 1 & \mathrm{e}^{\mathrm{i}\phi} \\ -\mathrm{e}^{-\mathrm{i}\phi} & 1 \end{pmatrix}. \tag{2}$$

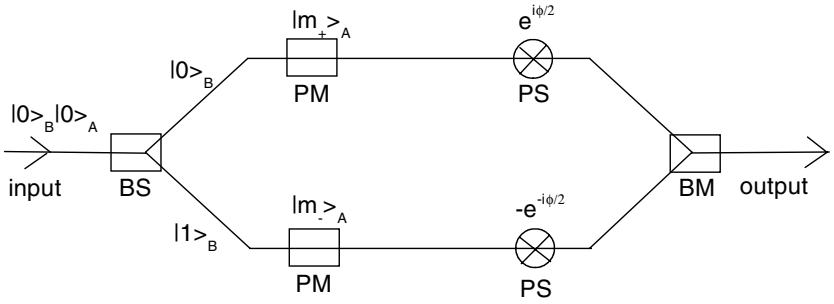

Figure 1. Schematic diagram of a two-way interferometer. The input, say $|0\rangle_B|0\rangle_A$, is split two ways by the beam splitter (BS), then labelled by the path markers (PM), phase shifted by the phase shifters (PS) and finally recombined into the output by the beam merger (BM).

And the output state $|\psi_2\rangle = U_2|\psi_1\rangle$ could be read as

$$|\psi_2\rangle = \tfrac{1}{2}[|0\rangle_B(|m_+\rangle_A + \mathrm{e}^{\mathrm{i}\phi}|m_-\rangle_A) + |1\rangle_B(|m_-\rangle_A - \mathrm{e}^{-\mathrm{i}\phi}|m_+\rangle_A)]. \tag{3}$$

Finally, measuring the population, I, of B in the states $|0\rangle_B$ and $|1\rangle_B$ gives

$$I(\phi) = \tfrac{1}{2}(1 \pm \mathrm{Re}({}_A\langle m_+|m_-\rangle_A)\,\mathrm{e}^{\mathrm{i}\phi}) \tag{4}$$

where '$\pm$' correspond to the populations in $|0\rangle_B$ and $|1\rangle_B$, respectively. Repeating the measurements at different ϕ might produce population fringes. Suppose the marker states $|m_\pm\rangle_A = \cos\varphi_\pm|0\rangle_A + \sin\varphi_\pm|1\rangle_A$, and from the usual definition of the fringe visibility $V = (I_{\max} - I_{\min})/(I_{\max} + I_{\min})$ and equation (4), one gets

$$V = |{}_A\langle m_+|m_-\rangle_A| = |\cos\varphi| \tag{5}$$

where $\varphi = \varphi_- - \varphi_+$.

Englert [2] proposed a quantitative measure for D by introducing a physical quantity L_W—the 'likelihood for guessing the right way', which depends on the choice of an observable W,

$$L_W = \sum_i \max\{p(W_i, |0\rangle_B),\, p(W_i, |1\rangle_B)\} \tag{6}$$

where $p\,(W_i, |0\rangle_B)$ and $p\,(W_i, |1\rangle_B)$ denote the joint probabilities that the eigenvalue W_i of W is found and the observed object takes path $|0\rangle_B$ or $|1\rangle_B$. For example, for the state of equation (1), an optimal observable W_{opt} can be found to maximize $L_W = (1 + |\sin\varphi|)/2$ in the experiments [21] and by the definition of the distinguishability D of paths $D = -1 + 2\max_W\{L_W\}$ [2], one gets

$$D(\varphi) = |\sin\varphi|. \tag{7}$$

Here, we present an expression for D in an intuitively geometric way. To this end, one projects the marker states $|m_\pm\rangle_A$ into an appropriate orthonormal basis $\{|\beta_+\rangle_A, |\beta_-\rangle_A\}$,

$$|m_+\rangle_A = \gamma_+|\beta_+\rangle_A + \gamma_-|\beta_-\rangle_A \qquad |m_-\rangle_A = \delta_+|\beta_+\rangle_A + \delta_-|\beta_-\rangle_A \tag{8}$$

where $|\gamma_+|^2 + |\gamma_-|^2 = |\delta_+|^2 + |\delta_-|^2 = 1$. In the two-path case, the criterion of choosing $\{|\beta_+\rangle_A, |\beta_-\rangle_A\}$ is to make the difference of probabilities of measuring the two states $|m_+\rangle_A$ and $|m_-\rangle_A$ on the basis $|\beta_+\rangle_A$ equal to that when measuring $|m_+\rangle_A$ and $|m_-\rangle_A$ on $|\beta_-\rangle_A$. These probability differences are then defined as the distinguishability

$$D = ||\gamma_+|^2 - |\delta_+|^2| = ||\delta_-|^2 - |\gamma_-|^2|. \tag{9}$$

The basis $\{|\beta_+\rangle_A, |\beta_-\rangle_A\}$ can be rewritten into the computational basis,

$$|\beta_+\rangle_A = \cos\theta|0\rangle_A + \sin\theta|1\rangle_A \qquad |\beta_-\rangle_A = \sin\theta|0\rangle_A - \cos\theta|1\rangle_A \tag{10}$$

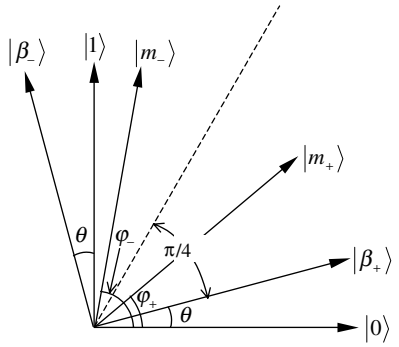

Figure 2. The state vectors in Hilbert space for defining D. $\{|0\rangle, |1\rangle\}$ represents the standard orthonormal basis. Two marker states $\{|m_\pm\rangle\}$ and another orthonormal basis $\{|\beta_\pm\rangle\}$ are determined by the angles φ_+, φ_- and θ, $\frac{\pi}{2}+\theta$, respectively. The dashed line denotes the angle bisector between the two states $\{|m_\pm\rangle\}$. From the map, one can get the relation $\theta = \frac{\varphi_+ + \varphi_-}{2} - \frac{\pi}{4}$.

where θ is the angle of the state vector $|\beta_+\rangle_A$ with respect to the basis $|0\rangle_A$. In order to satisfy equation (9), from figure 2 and by geometric knowledge $\theta = \frac{\varphi_+ + \varphi_-}{2} - \frac{\pi}{4}$ must hold, which yields

$$\gamma_+ = \delta_- = \cos\left(\frac{\pi}{4} - \frac{\varphi}{2}\right) \qquad \gamma_- = \delta_+ = \sin\left(\frac{\pi}{4} - \frac{\varphi}{2}\right). \tag{11}$$

Here, $\varphi = \varphi_- - \varphi_+$ is the angle between the two-marker-state vectors in Hilbert space. So from equations (9) and (11), the distinguishability is equally given by equation (7). It can also be seen that the desired basis $\{|\beta_+\rangle_A, |\beta_-\rangle_A\}$ deduced by our geometric strategy is just the eigenvectors of the optimal observable W_{opt} [21].

These expressions for V and D are consistent with those in [21] and lead to the duality relation

$$D^2(\varphi) + V^2(\varphi) = 1. \tag{12}$$

Equations (5) and (7) reveal the sinusoidal and cosinusoidal behaviours of D and V, respectively, on the angle φ between $|m_+\rangle_A$ and $|m_-\rangle_A$ in the Hilbert space H_A. D and V, therefore, are determined by the feature of $|m_+\rangle_A$ and $|m_-\rangle_A$, especially by the value of φ. However, for any value of φ the duality relation (13) holds when two evolution paths, $|0\rangle_B$ and $|1\rangle_B$, are labelled by quantum pure states $|m_+\rangle_A$ and $|m_-\rangle_A$. Generally equation (12) should be replaced by $D^2 + V^2 \leqslant 1$ [2, 15, 16].

As WW information of the observed system B is stored in the states of the marker system A through the interaction and correlation of A and B, the distinguishability of B's paths depends on the feature of the marker states, or more exactly, the correlation property of the combined system AB. It would be natural to examine the relationship between the entanglement of the system AB and the distinguishability. For a bipartite pure state, the entanglement E can be denoted by the von Neumann entropy S [24], $S = S(\rho^{(A)}) = S(\rho^{(B)})$, with $S(\rho^{A(B)}) = -\operatorname{Tr}(\rho^{A(B)} \log_2 \rho^{A(B)})$ and $\rho^{A(B)} = \operatorname{Tr}_{A(B)}(\rho_{AB})$ for each subsystem. The entanglement E for the pure state $|\psi_1\rangle$ shown in equation (1) is then derived as

$$E(\varphi) = -\frac{1-\cos\varphi}{2}\log_2\left(\frac{1-\cos\varphi}{2}\right) - \frac{1+\cos\varphi}{2}\log_2\left(\frac{1+\cos\varphi}{2}\right). \tag{13}$$

It can be obtained from equation (13) that $E = 0$ for $\varphi = k\pi$ and $E = 1$ for $\varphi = (2k+1)\pi/2$ with $k = 0, 1, 2, \ldots$, which correspond to $D = 0$ and 1, respectively. A detailed quantitative analysis of E will be given later (see figure 4).

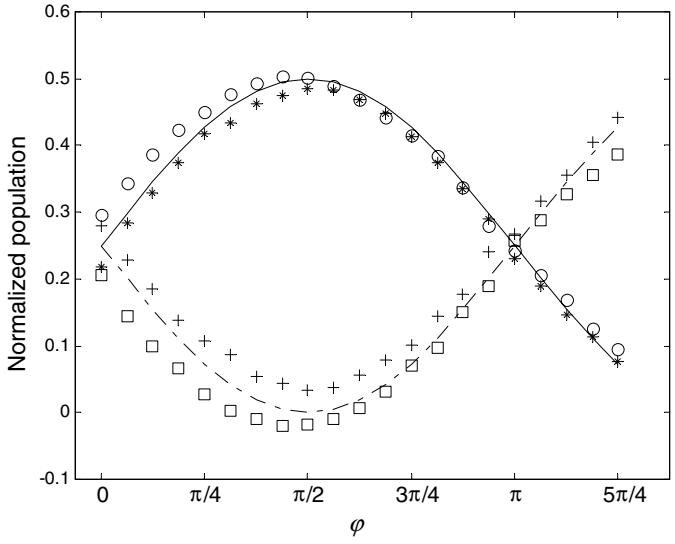

Figure 3. Normalized populations versus the angle φ, between two marker states in the experiments to measure D. Data points +, ◯, ∗ and ⊡ denote the joint probabilities $p(|\beta_+\rangle_A, |0\rangle_B)$, $p(|\beta_-\rangle_A, |0\rangle_B)$, $p(|\beta_+\rangle_A, |1\rangle_B)$ and $p(|\beta_-\rangle_A, |1\rangle_B)$, respectively. Theoretical curves expressed by $p(|\beta_+\rangle_A, |0\rangle_B) = p(|\beta_-\rangle_A, |1\rangle_B) = |\cos(\frac{\pi}{4} - \frac{\varphi}{2})|^2/2$ and $p(|\beta_-\rangle_A, |0\rangle_B) = p(|\beta_+\rangle_A, |1\rangle_B) = |\sin(\frac{\pi}{4} - \frac{\varphi}{2})|^2/2$ are depicted with the solid line and the dash-dotted line, respectively.

3. Experimental procedure and results

The scheme stated above was implemented by liquid-state NMR spectroscopy with a two-spin sample of carbon-13 labelled chloroform $^{13}CHCl_3$ (Cambridge Isotope Laboratories, Inc.). We made use of the hydrogen nucleus (^{1}H) as the marker spin A and the carbon nuclei (^{13}C) as the observed spin B in the experiments. Spectra were recorded on a BrukerARX500 spectrometer with a probe tuned at 125.77 MHz for ^{13}C and at 500.13 MHz for ^{1}H. The spin–spin coupling constant J between ^{13}C and ^{1}H is 214.95 Hz. The relaxation times were measured to be $T_1 = 4.8$ s and $T_2 = 3.3$ s for the proton, and $T_1 = 17.2$ s and $T_2 = 0.35$ s for carbon nuclei.

First, we prepared the quantum ensemble in an effective pure state ρ_0 from the thermal equilibrium by line-selective pulses with appropriate frequencies and rotation angles and a magnetic gradient pulse [25]. The state ρ_0 has the same properties and NMR experimental results as the pure state $|\psi_0\rangle = |00\rangle$. Then we transferred ρ_0 to another state ρ_1 equivalent to the state $|\psi_1\rangle$ shown in equation (1) for accomplishing the BS and PM actions by applying a Hadamard transformation $H_B = \frac{1}{\sqrt{2}}\begin{pmatrix}1 & 1\\ 1 & -1\end{pmatrix}$ on spin B and two unitary transformations

$$P_1 = \exp\left(-\mathrm{i}E_+^A\sigma_y^B\varphi_+\right) \qquad P_2 = \exp\left(-\mathrm{i}E_-^A\sigma_y^B\varphi_-\right) \tag{14}$$

where $\sigma_\eta^i(\eta = x, y, z)$ are Pauli matrices of the spin i, $E_\pm^i = \frac{1}{2}\left(1_2 \pm \sigma_z^i\right)$ and 1_2 is the 2×2 unit matrix. These operations were implemented by the NMR pulse sequence $Y_A(\varphi_+ + \varphi_-)X_A\left(\frac{\pi}{2}\right)J_{AB}(\varphi_- - \varphi_+)X_A\left(-\frac{\pi}{2}\right)X_B(\pi)Y_B\left(\frac{\pi}{2}\right)$ to be read from left to right, where $Y_A(\varphi_+ + \varphi_-)$ denotes an $\varphi_+ + \varphi_-$ rotation about $\hat{y}$-axis on spin A and so forth, and $J_{AB}(\varphi_- - \varphi_+)$ represents a time evolution of $(\varphi_- - \varphi_+)/\pi J_{AB}$ under the scalar coupling between spins A and B. Finally, the PS and BM operations were achieved by the transformation U_2,

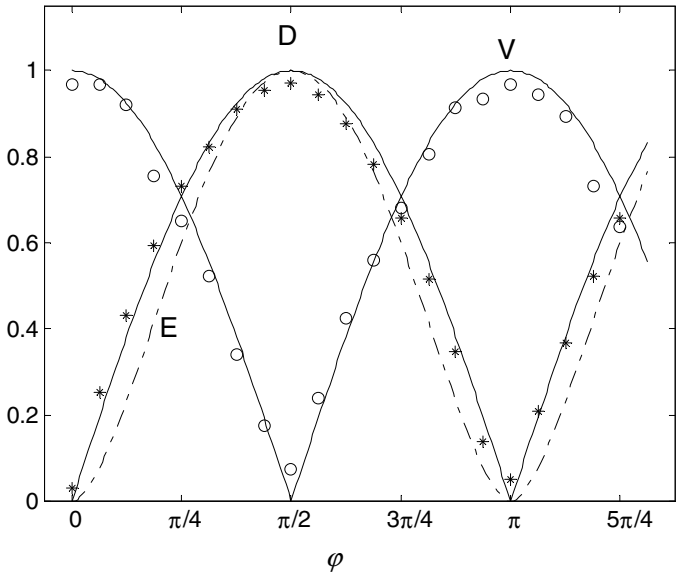

Figure 4. Visibility V (denoted by ◯) and distinguishability D (denoted by $*$) as a function of φ. The solid lines are the theoretical expectations of V and D and the dashed line denotes E expressed by equation (11).

which was realized by the NMR pulse sequence $X_B(-\theta_1)Y_B(\theta_2)X_B(-\theta_1)$ with $\theta_1 = \tan^{-1}(-\sin\phi)$, and $\theta_2 = 2\sin^{-1}(-\cos\phi/\sqrt{2})$.

In our experiments, two sets of experiments for a given value of $\varphi = \varphi_- - \varphi_+$ were performed to measure the fringe visibility V and the distinguishability D. In the experiment of a quantitative measure for D, whether it is defined by the geometric way or the maximum likelihood estimation, the joint probabilities $p(|\beta_\pm\rangle_A, |0\rangle_B)$ and $p(|\beta_\pm\rangle_A, |1\rangle_B)$ must be measured first. We performed the joint measurements by a two-part procedure inspired by Brassard *et al* [26]. Part one of the procedure is to rotate from the basis $\{|0\rangle_B|\beta_+\rangle_A, |0\rangle_B|\beta_-\rangle_A, |1\rangle_B|\beta_+\rangle_A, |1\rangle_B|\beta_-\rangle_A\}$ into the computational basis $\{|00\rangle, |01\rangle, |10\rangle, |11\rangle\}$ (omitting the subscripts A and B), which was realized by the unitary operation

$$R_B = \begin{pmatrix} \cos\alpha & -\sin\alpha \\ \sin\alpha & \cos\alpha \end{pmatrix} \tag{15}$$

where $\alpha = \frac{\pi}{4} - \frac{\varphi_+ + \varphi_-}{2}$, corresponding to the NMR pulse $Y_B(2\alpha)$. Part two of the procedure is to perform a projective measurement in the computational basis which could be simulated by a magnetic gradient pulse along the z-axis [27]. Accordingly, the joint probabilities $p(|\beta_\pm\rangle_A, |0\rangle_B)$ and $p(|\beta_\pm\rangle_A, |1\rangle_B)$ were obtained by reconstructing the diagonal elements of the deviation density matrix by quantum state tomography [28]. The results are shown in figure 3. In our geometric strategy, from equations (1) and (8) the information γ_+, γ_- or δ_+, δ_- can be obtained, determined by the population probabilities, i.e., $|\gamma_+|^2 = 2p(|0\rangle_B|\beta_+\rangle_A)$, $|\gamma_-|^2 = 2p(|0\rangle_B|\beta_-\rangle_A)$ and $|\delta_+|^2 = 2p(|1\rangle_B|\beta_+\rangle_A)$, $|\delta_-|^2 = 2p(|1\rangle_B|\beta_-\rangle_A)$. Finally, we used equation (9) and took the average value of $(||\gamma_+|^2 - |\delta_+|^2| + ||\delta_-|^2 - |\gamma_-|^2|)/2$ to give data points of D which are shown in figure 4. On the other hand, utilizing the data points of figure 3, we achieved the experimental values of the likelihood L_W from equation (6) and obtained the D measure with the maximum likelihood estimation strategy, which are the same outcomes as in

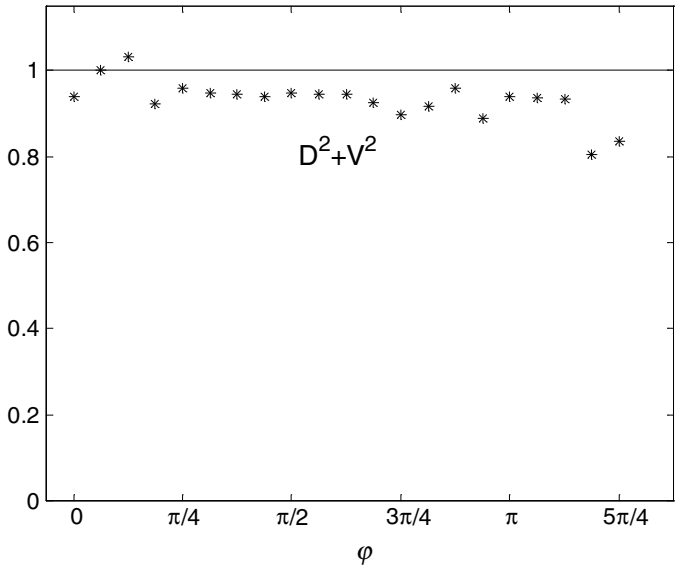

Figure 5. Experimental test of the duality relation based on the data from figure 3. $D^2 + V^2$ is plotted as a function of φ. The solid line represents the theoretical expectation.

our geometric strategy. Therefore, the intuitively geometric strategy gives an equally effective measure of the distinguishability D.

For measuring V, we repeatedly applied the NMR pulse sequence $X_B(-\theta_1)\,Y_B(\theta_2)\,X_B(-\theta_1)$ that represents the $U_2(\phi)$ operation for various values of ϕ and detected the population of B in the state ρ_2 equivalent to the output state $|\psi_2\rangle$. A set of appropriate values θ_1 and θ_2 were chosen to vary the values for ϕ from 0 to 2π. Using the same read-out pulses and tomography method as that in the measurement of D, we reconstructed the populations of B for various values of ϕ . The variation of the normalized populations versus ϕ showed a desirable interference fringe, from which the value of V was extracted. Care should be exercised in processing the spectra data of the different experimental runs in order to get the normalized populations of the deviation density matrix.

The objective of the present paper is to study the interferometric complementarity in the intermediate regime with two non-orthogonal marker states, so the experimental procedure mentioned above was repeated for different φ. Without loss of generality, we assumed $\varphi_+ = \frac{\pi}{2}$ and changed the φ values from 0 to $5\pi/4$ by varying the φ_- value with increments of $\pi/16$. The measured values of $V(\varphi)$ and $D(\varphi)$ in two sets of independent experiments were plotted in figure 4, along with the theoretical curves of $V(\varphi)$, $D(\varphi)$ and $E(\varphi)$. The experimental data and theoretical curve for $D^2(\varphi) + V^2(\varphi)$ are depicted in figure 5 (see figure 5).

From figures 4 and 5, some remarks can be made as follows.

(1) For $\varphi = k\pi$ ($k = 0, 1, 2, \ldots$), which means $|_A\langle m_+|m_-\rangle_A| = 1$, two marker states are identical (differing with an irrelevant phase factor possible), and the state of the system AB is completely unentangled ($E = 0$). In this case, no WW information of system B is stored in system A so that two evolution paths of B are indistinguishable ($D = 0$) and perfect fringe visibility is observed ($V = 1$). For $\varphi = (2k+1)\pi/2$, i.e., $|_A\langle m_+|m_-\rangle_A| = 0$, the marker states are orthogonal, and the state of the system AB is completely entangled ($E = 1$). This leads to full WW information ($D = 1$) and no interference fringes

($V = 0$). These two extremes are exactly the same examples that we have studied in [8] with an NMR bulk ensemble by population measurements.

(2) When φ equals other values than $k\pi$ and $(2k + 1)\pi/2$, which corresponds to $0 < |_A\langle m_+|m_-\rangle_A| < 1$, the marker states are partially orthogonal, and the state of the AB system is partially entangled ($0 < E < 1$). In these intermediate situations, partial fringe visibility ($0 < V < 1$) and partial WW information ($0 < D < 1$) result. Nevertheless, the interferometric duality still holds as in the extreme cases.

(3) In the whole range of φ, E varies synchronously with D. The reason is that the increase of E means more correlation between systems B and A and more WW information of B stored in A, so D rises, and vice versa. In contrast, the variation trend of E versus φ is opposite to that of V versus φ. As the function of E versus φ has a complicated form, there is no similar relation between E and V to the duality of $D^2 + V^2 = 1$.

(4) The measured values of V, D and thus the derived values of D^2+V^2 are fairly in agreement with theoretical expectation. The discrepancies between the experimental and theoretical values of V, D and $D^2 + V^2$ at some data points, estimated to be less than $\pm 10\%$, are due to the inhomogeneity of the RF field and static magnetic field, imperfect calibration of RF pulses, and signal decay during the experiments.

4. Conclusion

In conclusion, we have experimentally tested the interferometric complementarity in a spin ensemble with NMR techniques. In addition to two extremes, the intermediate cases that the fringe visibility V reduces due to increase in the storage of WW information are emphasized. The measured data of D and V in our NMR experiments are consistent with the duality relation. In particular, the close link among D, V and the entanglement of the composite system consisting of the observed and marker states is explicitly revealed and explained. Though the experiment was not strictly limited in the one-photon-at-a-time fact, it was performed on a quantum ensemble whose dynamical evolution is still quantum-mechanical. Therefore, our experiment provides a test of the duality relation in the intermediate situations.

Acknowledgments

This work was supported by the National Natural Science Foundation of China (grant no 1990413). XP thanks Xiaodong Yang, Hanzeng Yuan and Xu Zhang for their help in the course of the experiments.

References

[1] Bohr N 1928 *Naturwissenschaften* **16** 245
Bohr N 1928 *Nature* **121** 580
[2] Englert B-G 1996 *Phys. Rev. Lett.* **77** 2154
[3] Feynman R P, Leifhton R B and Sands M 1965 *The Feynman Lectures of Physics, Vol III. Quantum Mechanics* (Reading, MA: Addison-Wesley)
[4] Taylor G I 1909 *Proc. Camb. Phil. Soc.* **15** 114
[5] Möllenstedt G and Jönsson C 1959 *Z. Phys.* **155** 472
Tonomura A, Endo J, Matsuda T and Kawasaki T 1989 *Am. J. Phys.* **57** 117
[6] Zeilinger A, Gähler R, Shull C G, Treimer W and Mampe W 1988 *Rev. Mod. Phys.* **60** 1067
[7] Carnal O and Mlynek J 1991 *Phys. Rev. Lett.* **66** 2689
[8] Zhu X, Fang X, Peng X, Feng M, Gao K and Du F 2001 *J. Phys. B: At. Mol. Opt. Phys.* **34** 4349

[9] Bohr N 1949 *Albert Einstein: Philosopher Scientist* ed P A Schilpp (Evanston, IL: Library of Living Philosophers) pp 200–41
Reprinted in 1983 *Quantum Theory and Measurement* ed J A Wheeler and W H Zurek (Princeton, NJ: Princeton University Press) pp 9–49
[10] Scully M O, Englert B-G and Walther H 1991 *Nature* **351** 111
[11] Wootters W K and Zurek W H 1979 *Phys. Rev.* D **19** 473
[12] Bartell L S 1980 *Phys. Rev.* D **21** 1698
[13] Greenberger D M and Yasin A 1988 *Phys. Lett.* A **128** 391
[14] Mandel L 1991 *Opt. Lett.* **16** 1882
[15] Jaeger G, Shimony A and Vaidman L 1995 *Phys. Rev.* A **51** 54
[16] Englert B-G and Bergou J A 2000 *Opt. Commun.* **179** 337
[17] Rauch H and Summhammer J 1984 *Phys. Lett.* A **104** 44
[18] Summhammer J, Rauch H and Tuppinger D 1987 *Phys. Rev.* A **36** 4447
[19] Mittelstaedt P, Prieur A and Schieder R 1987 *Found. Phys.* **17** 891
[20] Schwindt P D D, Kwiat P G and Englert B-G 1999 *Phys. Rev.* A **60** 4285
[21] Dürr S, Nonn T and Rempe G 1998 *Phys. Rev. Lett.* **81** 5705
[22] Bertet P, Osnaghl S, Rauschenbeutel A, Nogues G, Auffeves A, Brune M, Ralmond J M and Haroche S 2001 *Nature* **411** 166
[23] Scully M O and Zubairy M S 1997 *Quantum Optics* (Cambridge: Cambridge University Press)
[24] Bennett C H, Bernstein H J, Popescu S and Schumacher B 1996 *Phys. Rev.* A **53** 2046
[25] Peng X, Zhu X, Fang X, Feng M, Gao K, Yang X and Liu M 2001 *Chem. Phys. Lett.* **340** 509
[26] Brassard G, Braunstein S and Cleve R 1998 *Physica* D **120** 43
[27] Teklemariam G, Fortunato E M, Pravia M A, Havel T F and Cory D G 2001 *Phys. Rev. Lett.* **86** 5845
[28] Chuang I L, Gershenfeld N, Kubinec M and Leung D 1998 *Proc. R. Soc.* A **454** 447